Identification and attenuation of Scholte waves in shallow water seismic data from Pelotas basin

Vinicius José Oliveira Werneck de Carvalho, Marco Cetale, Ursula Belem da Silva, Guilherme Henrique Lenz, Roberto Miyamoto Pessoa and Taís Renata Zanato, UFF/DOT/GISIS.

This paper was prepared for presentation during the 17th International Congress of the Brazilian Geophysical Society held in Rio de Janeiro, Brazil, 16-19 August 2021.

Abstract

The shallow water processing has its own characteristics, caused by the multiple reverberations caused by the shallow water blade. In addition to this peculiarity, data of this nature may present noise similar to the ground roll, called Scholte waves.

Scholte waves are, dispersive and slow waves, however, of great amplitude, which propagate along the seabed, which can mask reflections. In order to attenuate or remove Scholte waves, two different denoise methodologies were used in this work: F-K Filtering and LFAF (Low Frequency Array Filtering). Results, advantages and disadvantages were presented, leading to a comparative conclusion and information on the efficiency in attenuation of Scholtes waves. The data re-processed in this research are located in the Pelotas Basin, located in the extreme south of the Brazilian continental margin.

Introduction

The processed data comes from the Pelotas Basin, which is located in the southern region of the Brazilian east coast. This basin has a submerged area of 346.873 km², while the emersed region occupies approximately 40.900 km². The shallow part (water depth) is approximately 50 meters, while the deeper part can reach about 2 thousand meters in depth (Figure 1).

It is rich in magma, has a thick layer of lava spills plunging into the sea (SDR - seaward dipping reflections), has growth controlled by failures that plunge into the continent (Stica et al., 2014). The drift fill is characterized by retrogradation between the Cretaceous and the Paleogen and intense Neogenous progradation (CONTRERAS et al., 2010).

Its exploration began in 1958 and most of its seismic data was acquired between the 70s and 90s, however it remains little explored. The basin contains proven reserves of gas hydrate in the Cone of Rio Grande Province; however, it is still an exploratory frontier for oil (Miller et al., 2015). Recent studies point to possible reservations throughout the basin's stratigraphy, from the Uruguayan to the Brazilian portion (Conti et al., 2017 and Zalan et al., 2017).

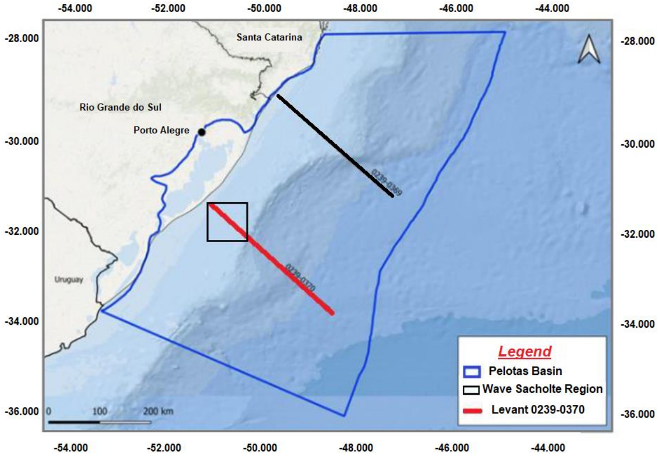

Figure 1. Location of the study area.

This work aims to present a methodology that can mitigate the interference of the Scholtes waves, improving the seismic interpretation, increasing the final quality of the processed data.

Theory

Shallow water processing has unique characteristics, such as reverberations, caused by the blade in shallow water, presenting noises similar to the ground roll, the so-called Scholte waves (Figure 1).

Along the seabed there is an interface that separates fluid and solid, and can generate two types of guide waves, Rayleigh waves and Scholte waves (Johansen et. Al. 2020). However, according to Johansen, the sediments of the seabed are very loose, causing the speed of the S wave (V_s) on the seabed to be greater than the acoustic speed of the water(V_w), that is, $(V_s \gg V_w)$, thus considering only the Scholte waves.

Its generation process can be attributed to the proximity of the source to the seabed, and can be directly excited by the source. However, there is another important generating mode, attributed to the topographic factor of the seabed, since the same is not necessarily flat (Sato, 2012).

The topography of the seabed can excite strong interface waves, which are usually dispersive and slow to propagate, but of great amplitude. The generation of Scholte waves was theoretically well understood in a flat interface (de Hoop and Van der Hijden, 1983, 1984). Hoop and Van der Hijden, concluded that Scholte waves can exist along the solid-liquid interface, satisfying the mathematical scalar model, with eight Riemann sheets owing to three square roots:

$$\frac{1}{4V_S^4}\frac{\rho_f\eta_P}{\rho_S\eta_f} + \left(P^2 - \frac{1}{2V_S^2}\right)^2 + P^2\eta_P\eta_S = 0, \qquad (1)$$

where V_s is the fluid velocity, η_f, η_p, η_S the compression and shear rates respectively of the underlying solids. The variables ρ_f e ρ_S are the densities of the fluid and the solid respectively and P the index of slowness of the medium. Here,

$$\eta_{f,P,S} = \sqrt{c_{f,P,S}^{-2} - P^2}, \qquad (2)$$

with

$$Re(\eta_{f,P,S}) \geq 0. \qquad (3)$$

When considering fluid and solid as two media in space, the speed of the Scholte wave, V_{sch}, is found (Vinh et al. 2013). The speed of propagation V_{sch}, is less than the speed of fluid and of the underlying solids, that is, $V_{sch} < \min(V_f, V_s, V_P)$. Johansen, in his study, states that $V_{sch} = 0.9V_s$ is a good approximation, frequently used (Johansen et al. 2019a).

The amplitude of the Scholte wave decays exponentially with the distance from the seabed. In shallow water, its resulting amplitude is modulated by the surface interference, which can impair the seismic interpretation, camouflaging or masking several features (Figure 2).

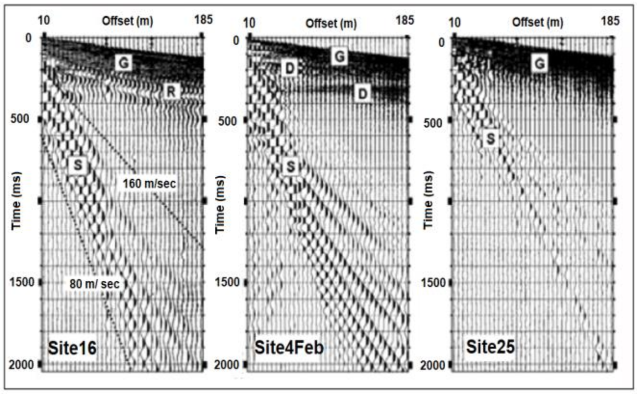

Figure 2. Examples of marine data records showing the Scholte (S), guide (G), refraction (R) and reflection (D) waves. Park, Choon B., et al. (2005), adapted.

Method

To attenuate or improve the quality of the seismic signal, due to the effects of the Scholtes waves, F-K Filtering and LFAF (Low Frequency Array Filtering) were used. The software used was Echos of Emerson, Paradigm^{TM}19.

The function of F-K Filtering is to design and apply filters in the $f-k, 2D$ domain, where f is the frequency and k is the wave number. With the change of domain $t-x \rightarrow f-k$, all data is mapped / presented differently. Thus, it is possible to 'isolate' some noise, facilitating the removal/attenuation, performing the separation according to the frequency and wave number.

For the reflections to be passed from the $t-x$ domain to the $f-k$, it is necessary to use the two-dimensional Fourier transform (F-K transform), given by the equation:

$$F(\omega, k_x) = \int_{-\infty}^{\infty}\int_{-\infty}^{\infty} f(t,x)e^{-ik_x\omega t}dtdx, \qquad (4)$$

The second method applied to attenuation of Scholtes waves in this work was the use of LFAF (Low Frequency Array Filtering). This method is related to the attenuation of surface waves by the matrix length (M), which depends on the frequency range $f \leq 25Hz$, the surface speed (V) and the spatial distance of the traces (D_x), exposed in the equation:

$$M = \frac{V}{Dx \times f}, \qquad (5)$$

Equation (5) changes the time-space domain to the frequency-space domain, which is directly associated with the specified frequency range.

Results

This section shows the results obtained through the methodology described above. Initially, we applied the F-K Filtering technique, in an attempt to attenuate or remove as much as possible the effects of the Scholte wave.

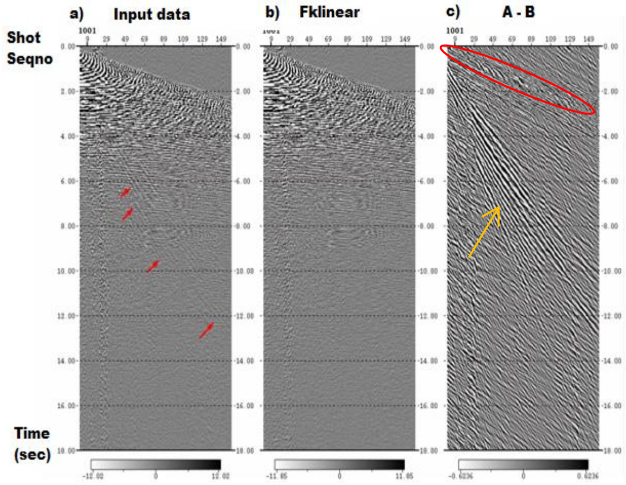

Figure 3. Image (a) input data, Scholte waves. (b) Fklinear applied and (c) difference between the input and output data, showing the Scholte waves that have been attenuated.

Figure 3a) illustrates the input data, showing the effect caused by the Scholte wave (smooth vertical lines, red arrows), while in Figure 3b), it shows the applied F-K Filtering. It is noticed that the Scholte waves were significantly attenuated (A-B), Figure 3c). However, a slight attenuation was observed, possibly in the primary waves (red circle).

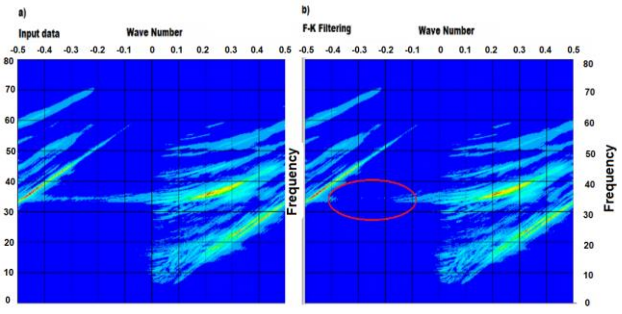

Figure 4. Spectral analysis of the input (a) and output (b) data.

The spectral analysis, Figure 4, showed a significant attenuation in the frequency range between 30 to 40 Hz, between the wave number - 0,4 to - 0,1. However, there was no energy change between 30 to 40Hz, in the 0,2 wave number.

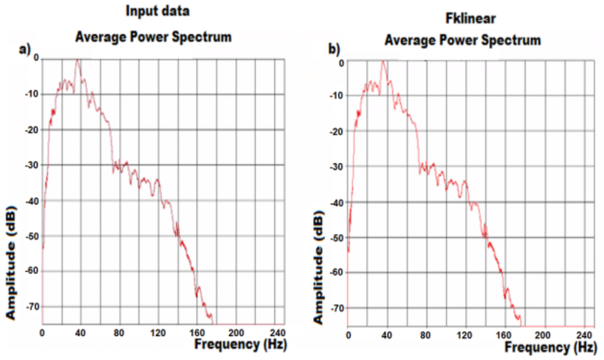

Figure 5. Power spectrum. Input (a) and output (b) data.

The results obtained in the power spectrum before and after, corroborate the results in the spectral analysis, showing absence of energetic anomalies (Figure 5). The input data presented the same spectral morphology as the output data (F-K Filtering). Both spectral analyzes started at - 3dB, with a maximum frequency recorded at 168 Hz.

The use of the LFAF method motivated a pre-analysis of the seismic data, making it possible to infer the average surface speed, in the value of 300 m / s and the frequency range from 0 to 8 Hz of the S wave. After this analysis, the LFAF method was applied, where a good attenuation of the Scholte waves was observed. However, it also came to possibly attenuate some primaries, in a more intense way, (red circle), Figure 6c.

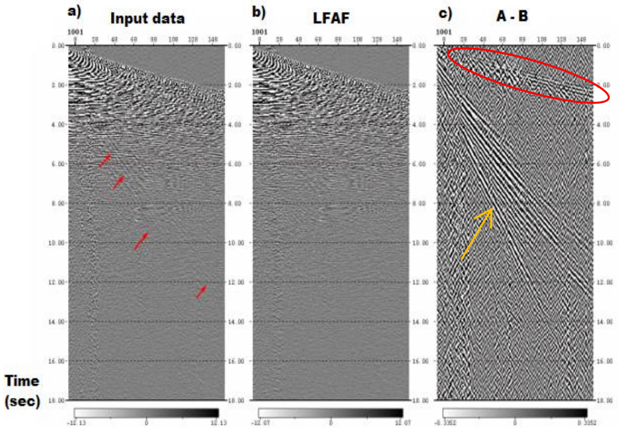

Figure 6: Image (a) input data, still under the effect of Scholte waves. (b) given with the LFAF and in the image (c), the difference between the input and output data (A - B).

Figure 7 shows the result of the spectral analysis before and after the LFAF procedure. After the procedure, a slight attenuation in energy was observed (red arrow) compared to the input data, in the region of 40 Hz, between 0,2 and 0,3.

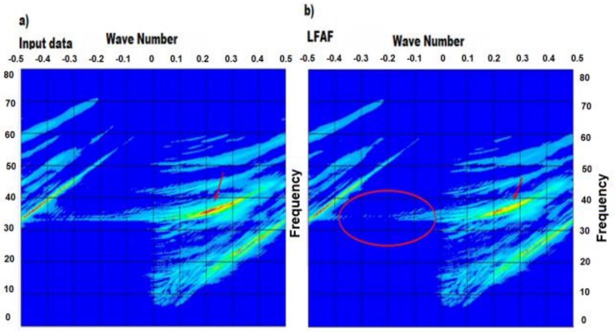

Figure 7: Analysis in the F-K domain. Input data (a), and after applying the LFAF (b).

In the 30 Hz range, energy attenuation or suppression (red circle) between - 0,4 and - 0,1 was also observed.

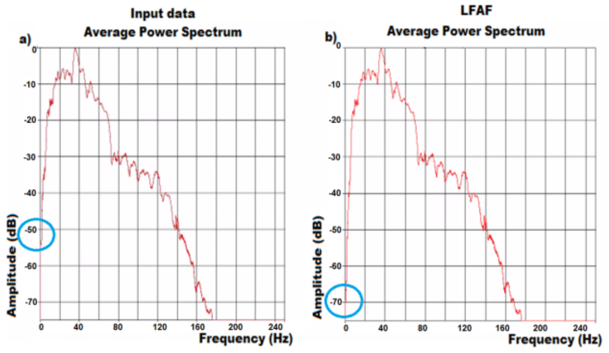

Figure 8. Spectral analysis of the input data (a) and the LFAF output data (b).

The power spectrum (Figure 8), presented similar spectral morphologies before and after. However, the power spectrum of the LFAF showed an initial amplitude of -50 dB, while in the input data, - 65dB. Result that possibly is correlated to that of Figure 7, regarding the energy attenuation found. Figure 9 shows the specifications used for F-K Filtering and LFAF, respectively.

F-K Filtering	K	F
[0]	0.097466	4.302716
[1]	0.5	20.87275
[2]	0.5	2.014037
[3]	0	1.159597
[4]	0.087719	3.722917
[5]	0.097466	4.302716

Table 1: Filtering parameters F-K filtering, polygon - wavenumber-frequency filter specifications.

Parameters	LFAF
0	Lowest frequency of the noise to be attenuated (F1).
8	Highest frequency of the noise to be attenuated (F2).
300	Surface wave velocity (VEL).
0	Spatial sampling interval (DX).
5	Frequency taper lenght (FTAPER).
0	Largest number of traces to be mixed (MAXMIX).

Table 2: Filtering specifications LFAF.

Conclusions

After presenting the results, it is concluded that both methodologies (Fklinear and LFAF) achieved good results in mitigating the effects of the Scholte wave. As a result, the aforementioned methodologies were able to reduce the effects of these waves, which previously masked and impaired the final seismic result.

However, F-K Filtering showed advantages in the physical conservation of data, as shown in the spectral analysis (Figure 4) and in the power spectrum (Figure 5). We can conclude that F-K Filtering obtained a better performance in the process of transformation of domains (t - x →f - k), than LFAF, not generating or suppressing any relevant signal. Both the F-K Filtering and the LFAF have managed to mitigate some primary waves. However, it was observed that the LFAF attenuated more intensely.

It is concluded that for this type of processed data, both methodologies fulfill the function well in attenuating the Scholte wave, with an advantage for F-K Filtering.

Acknowledgments

We would like to thank PETROBRAS for the financial support. We want to express my thanks to ANP (National Petroleum Agency). We also acknowledge Emerson-Paradigm for the technical support and the academic license processing software. We would like to thank GISIS group and to UFF's infrastructure.

References

Conti, Bruno, et al. "Speculative petroleum systems of the southern Pelotas Basin, offshore Uruguay." Marine and Petroleum Geology 83 (2017): 1-25.

CONTRERAS, J. et al. Seismic stratigraphy and subsidence analysis of the southern brazilian margin (campos, santos and pelotas basins). *Marine and Petroleum Geology*, Elsevier BV, v. 27, n. 9, p. 1952–1980, out. 2010. Disponível em:

<https://doi.org/10.1016/j.marpetgeo.2010.06.007>.

Hoop, Adrianus T., and Jos HMT Van der Hijden. "Generation of acoustic waves by an impulsive point source in a fluid/solid configuration with a plane boundary." The Journal of the Acoustical Society of America 75.6 (1984): 1709-1715.

Johansen, Tor Arne, and Bent Ole Ruud. "Characterization of seabed properties from Scholte waves acquired on floating ice on shallow water." Near Surface Geophysics 18.1-Quantitative Geophysical Characterization of Marine Near-Surface (2020): 49-59.

Miller, Dennis J., et al. "Natural gas hydrates in the Rio Grande Cone (Brazil): A new province in the western South Atlantic." Marine and Petroleum Geology 67 (2015): 187-196.

Muyzert, Everhard. "Seabed property estimation from ambient-noise recordings: Part 2—Scholte-wave spectral-ratio inversion." Geophysics 72.4 (2007): U47-U53.

Park, Choon B., et al. "Underwater MASW to evaluate stiffness of water-bottom sediments." The Leading Edge 24.7 (2005): 724-728.

Sato, Haruo, Michael C. Fehler, and Takuto Maeda. Seismic wave propagation and scattering in the heterogeneous earth. Vol. 496. Berlin: Springer, 2012.

Stica, Juliano Magalhães, Pedro Victor Zalán, and André Luiz Ferrari. "The evolution of rifting on the volcanic margin of the Pelotas Basin and the contextualization of the Paraná–Etendeka LIP in the separation of Gondwana in the South Atlantic." Marine and Petroleum Geology 50 (2014): 1-21.

Van Vossen, Robbert, Johan OA Robertsson, and Chris H. Chapman. "Finite-difference modeling of wave propagation in a fluid–solid configuration." Geophysics 67.2 (2002): 618-624.

Vinh, Pham Chi. "Scholte-wave velocity formulae." *Wave Motion* 50.2 (2013): 180-190.

Zalán, Pedro Victor. "Where Should We Drill in the Deep Waters of the Pelotas Basin, Southern Brazil and Uruguay." AAPG Centennial Annual Convention, AAPG Search and Discovery Article. Vol. 10975. 2017.

Zheng, Yingcai, et al. "Scholte waves generated by seafloor topography." arXiv preprint arXiv:1306.4383 (2013).